US008373175B1

(12) **United States Patent**
**Okojie**

(10) **Patent No.: US 8,373,175 B1**
(45) **Date of Patent: Feb. 12, 2013**

(54) **DUAL OHMIC CONTACT TO N- AND P-TYPE SILICON CARBIDE**

(75) Inventor: **Robert S. Okojie**, Cleveland, OH (US)

(73) Assignee: **The United States of America as represented by the Administrator of National Aeronautics and Space Administration**, Washington, DC (US)

( * ) Notice: Subject to any disclaimer, the term of this patent is extended or adjusted under 35 U.S.C. 154(b) by 3 days.

(21) Appl. No.: **12/791,276**

(22) Filed: **Jun. 1, 2010**

(51) **Int. Cl.**
***H01L 29/12*** (2006.01)

(52) **U.S. Cl.** ..... **257/77**; 257/E21.054

(58) **Field of Classification Search** ..... 257/77, 257/E21.054

See application file for complete search history.

(56) **References Cited**

U.S. PATENT DOCUMENTS

2006/0273323 A1* 12/2006 Yamamoto et al. ..... 257/77

OTHER PUBLICATIONS

Fursin et al. "Nickel ohmic contacts to p- and n-type 4H-SiC," Electronic letters vol. 37, p. 1092, Aug. 16, 2001.*

Tsukimoto et al. Simultaneous Formation of p- abd n-Type Ohmic Contacts to 4H-Sic using Ternary Ni/Ti/Al System, J. of Elec. Mat. vol. 34, p. 1310, 2006.*

* cited by examiner

*Primary Examiner* — Matthew Reames

(74) *Attorney, Agent, or Firm* — Robert H. Earp, III

(57) **ABSTRACT**

Simultaneous formation of electrical ohmic contacts to silicon carbide (SiC) semiconductor having donor and acceptor impurities (n- and p-type doping, respectively) is disclosed. The innovation provides for ohmic contacts formed on SiC layers having n- and p-doping at one process step during the fabrication of the semiconductor device. Further, the innovation provides a non-discriminatory, universal ohmic contact to both n- and p-type SiC, enhancing reliability of the specific contact resistivity when operated at temperatures in excess of 600° C.

**17 Claims, 24 Drawing Sheets**

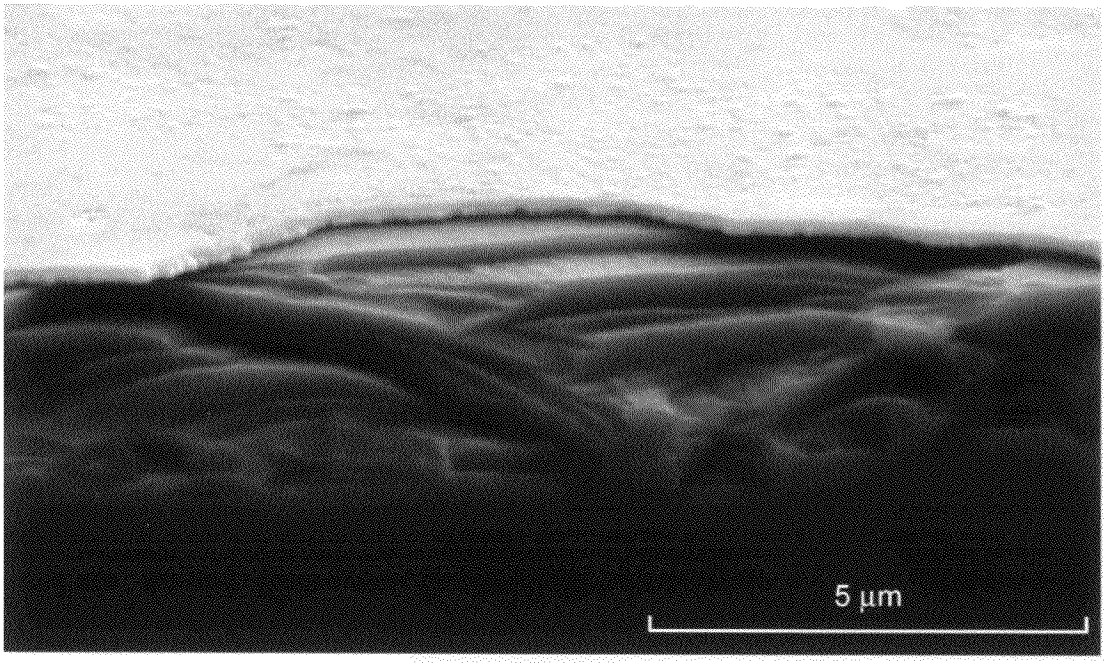

TABLE 1

| Sputtering conditions | | | |
|---|---|---|---|
| Pressure | 18.5 mTorr | Sputter time | 30 min |
| Spacing | ~5 in. | Pre-sputter | 20 min |
| Gas flow | 25 sccm | Power | 20 W RF |
| Chamber | UHV | Gun | 2 |
| UHV base | $6.1\times10^{-8}$ torr | DC bias 1 | –411 V (A) |
| UHV base | $7.7\times10^{-8}$ torr | DC bias 2 | –407 V (B) |
| UHV base | $8.2\times10^{-8}$ torr | DC bias 3 | –408 V (C) |

**Figure 1**

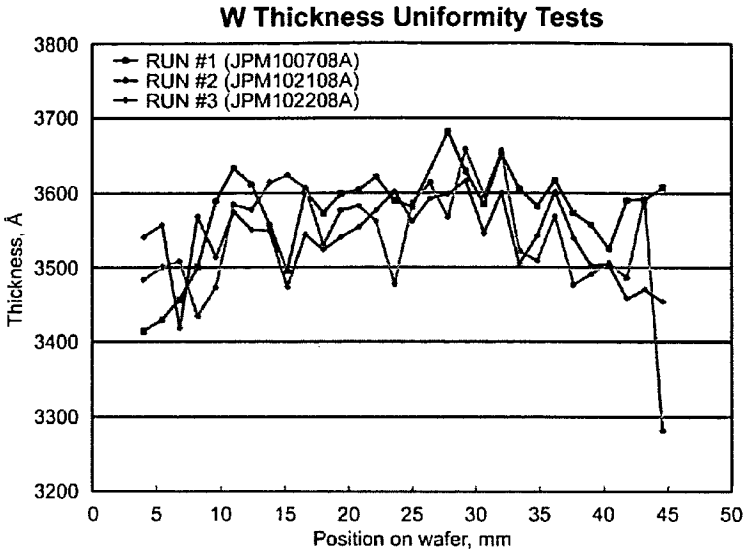


Table A

| | Run 1 n=30 | Run 2 n=30 | Run 3 n=30 | All runs n=90 |
|---|---|---|---|---|
| Mean (Å) | 3574 | 3542 | 3539 | 3552 |
| Std dev (Å) | 63 | 77 | 49 | 65 |
| Minimum (Å) | 3415 | 3281 | 3419 | 3281 |
| Maximum (Å) | 3682 | 3659 | 3616 | 3682 |
| Range (Å) | 268 | 377.4 | 197 | 401 |
| % error | 3.7 | 5.3 | 2.8 | 5.6 |

Table B

| | Run 1 n=30 | Run 2 n=30 | Run 3 n=30 | All runs n=90 |
|---|---|---|---|---|
| Mean (Å) | 1.99 | 1.97 | 1.97 | 1.97 |
| Std dev (Å) | 0.03 | 0.04 | 0.03 | 0.04 |
| Minimum (Å) | 1.90 | 1.82 | 1.90 | 1.82 |
| Maximum (Å) | 2.05 | 2.03 | 2.01 | 2.05 |
| Range (Å) | 0.15 | 0.21 | 0.11 | 0.22 |

Table C

| | Sputtering conditions | | |
|---|---|---|---|
| Pressure | 18.5 mTorr | Sputter time | 30 min |
| Spacing | ~5 in. | Pre-sputter | 20 min |
| Gas flow | 25 sccm | Power | 20 W RF |
| Chamber | UHV | Gun | 2 |
| UHV base | $6.1\times10^{-8}$ torr | DC bias 1 | –411 V |
| UHV base | $7.7\times10^{-8}$ torr | DC bias 2 | –407 V |
| UHV base | $8.2\times10^{-8}$ torr | DC bias 3 | –408 V |

Figure 2

TABLE 2

| Sputtering conditions | | | |
|---|---|---|---|
| Pressure | 3.5 mTorr | Sputter time | 1 hr |
| Spacing | ~5 in. | Presputter | 20 min |
| Gas flow | 25 sccm | Power | 20 W RF |
| Chamber | UHV | Gun | 1 |
| UHV base | $8.0\times10^{-8}$ torr | DC bias 1 | –404 V (A) |
| UHV base | $2.4\times10^{-7}$ torr | DC bias 2 | –406 V (B) |
| UHV base | $2.7\times10^{-7}$ torr | DC bias 3 | –406 V (C) |

**Figure 3**

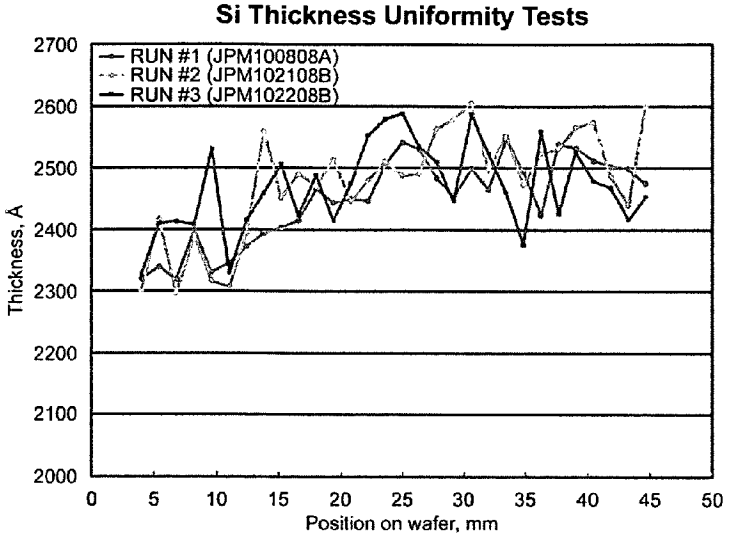


Table A

| | Run 1 n=30 | Run 2 n=30 | Run 3 n=30 | All runs n=90 |
|---|---|---|---|---|
| Mean (Å) | 2449 | 2478 | 2470 | 2466 |
| Std dev (Å) | 71 | 89 | 71 | 77 |
| Minimum (Å) | 2319 | 2296 | 2327 | 2296 |
| Maximum (Å) | 2547 | 2606 | 2589 | 2606 |
| Range (Å) | 228 | 310 | 261 | 310 |
| % error | 4.7 | 6.3 | 5.3 | 6.3 |

Table B

| | Run 1 n=30 | Run 2 n=30 | Run 3 n=30 | All runs n=90 |
|---|---|---|---|---|
| Mean (Å) | 0.68 | 0.69 | 0.69 | 0.68 |
| Std dev (Å) | 0.02 | 0.025 | 0.02 | 0.02146 |
| Minimum (Å) | 0.64 | 0.64 | 0.65 | 0.64 |
| Maximum (Å) | 0.71 | 0.72 | 0.72 | 0.72 |
| Range (Å) | 0.06 | 0.09 | 0.07 | 0.09 |

Table C

| | Sputtering conditions | | |
|---|---|---|---|
| Pressure | 3.5 mTorr | Sputter time | 1 hr |
| Spacing | ~5 in. | Presputter | 20 min |
| Gas flow | 25 sccm | Power | 20 W RF |
| Chamber | UHV | Gun | 1 |
| UHV base | $8.0\times10^{-8}$ torr | DC bias 1 | −404 V (A) |
| UHV base | $2.4\times10^{-7}$ torr | DC bias 2 | −406 V (B) |
| UHV base | $2.7\times10^{-7}$ torr | DC bias 3 | −406 V (C) |

**Figure 4**

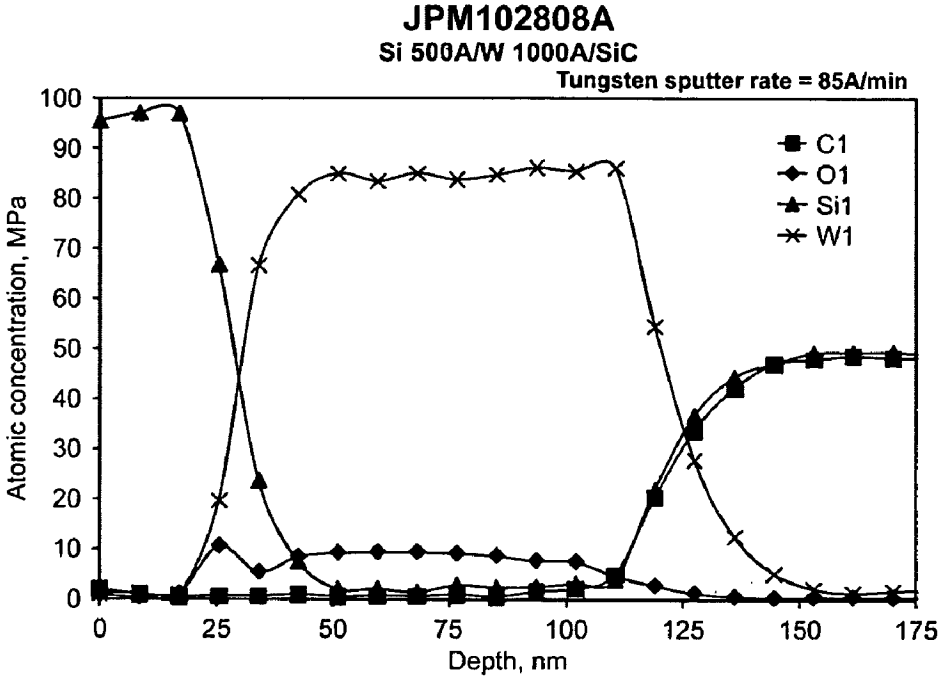
JPM102808A
Si 500A/W 1000A/SiC
Tungsten sputter rate = 85A/min
Atomic concentration, MPa
Depth, nm
C1
O1
Si1
W1
0
10
20
30
40
50
60
70
80
90
100
0
25
50
75
100
125
150
175

Figure 5

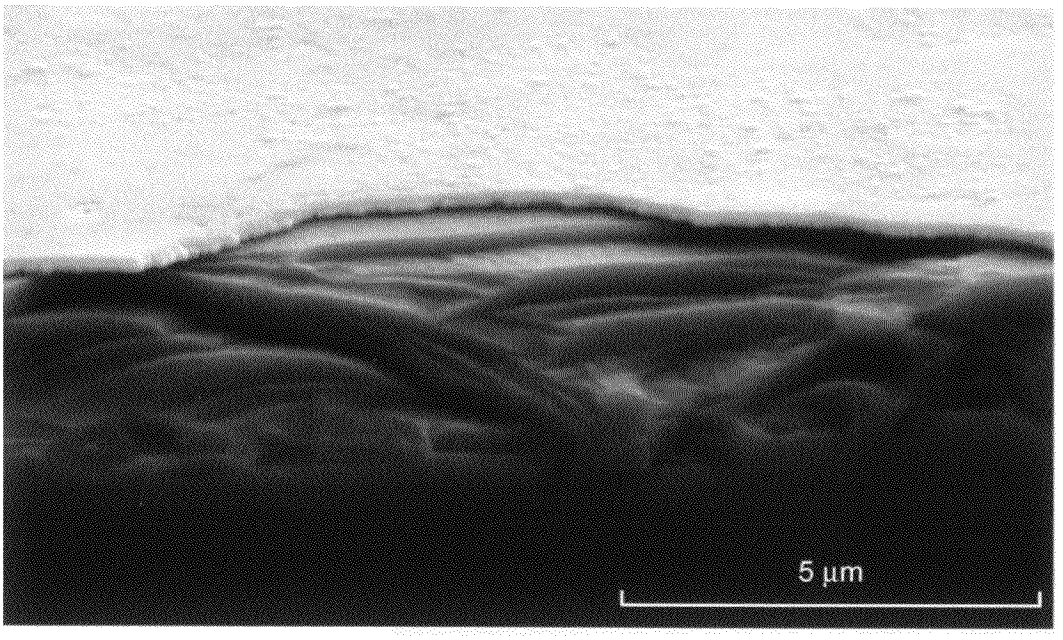


Figure 6

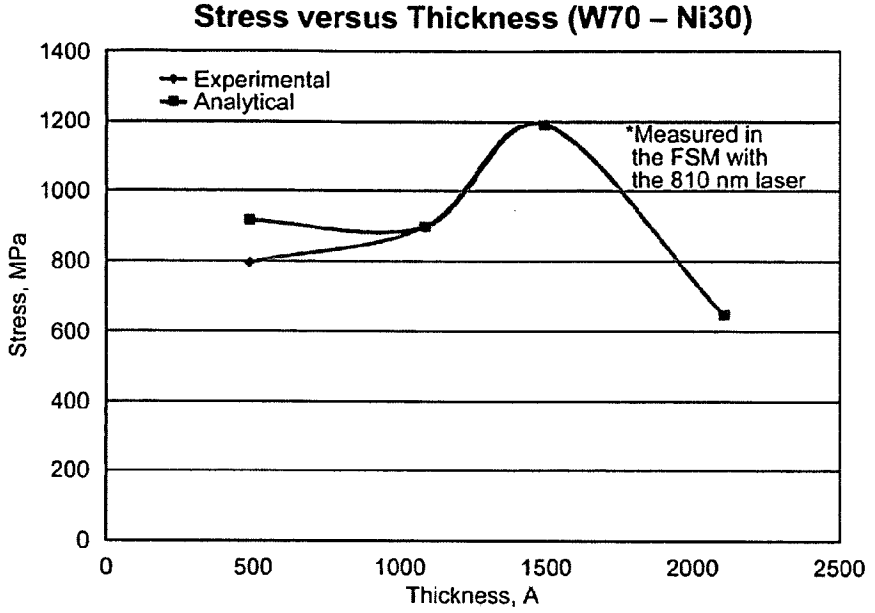


Table A

| W70–Ni30 Measured (810 nm laser) | |
|---|---|
| Thickness, Å | Stress, MPa |
| 488 | 796.5 |
| 1086 | 898.4 |
| 1494 | 1192 |
| 2105 | 645.7 |

Table B

| W70–Ni30 Calculated (810 nm laser) | |
|---|---|
| Thickness, Å | Stress, MPa |
| 488 | 918 |
| 1086 | 900 |
| 1494 | 1190 |
| 2105 | 647 |

Figure 7

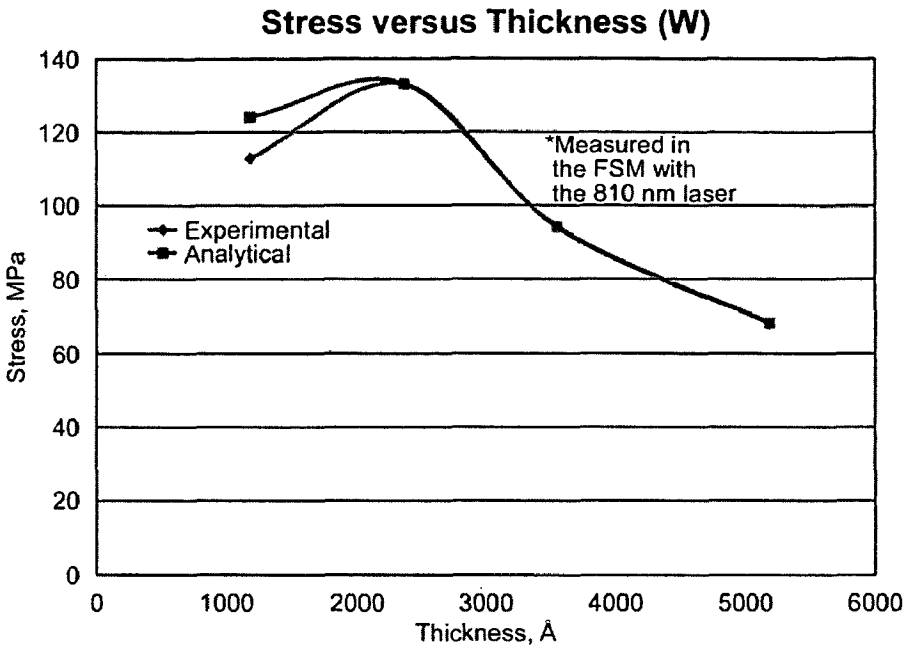


Table A

| W100% | |
|---|---|
| Measured (810 nm laser) | |
| Thickness, Å | Stress, MPa |
| 1182 | 113 |
| 2364 | 133.1 |
| 3546 | 94.16 |
| 5183 | 68.03 |

Table B

| W100% | |
|---|---|
| Calculated (810 nm laser) | |
| Thickness, Å | Stress, MPa |
| 1182 | 124 |
| 2364 | 133 |
| 3546 | 94.3 |
| 5183 | 68.15 |

Figure 8

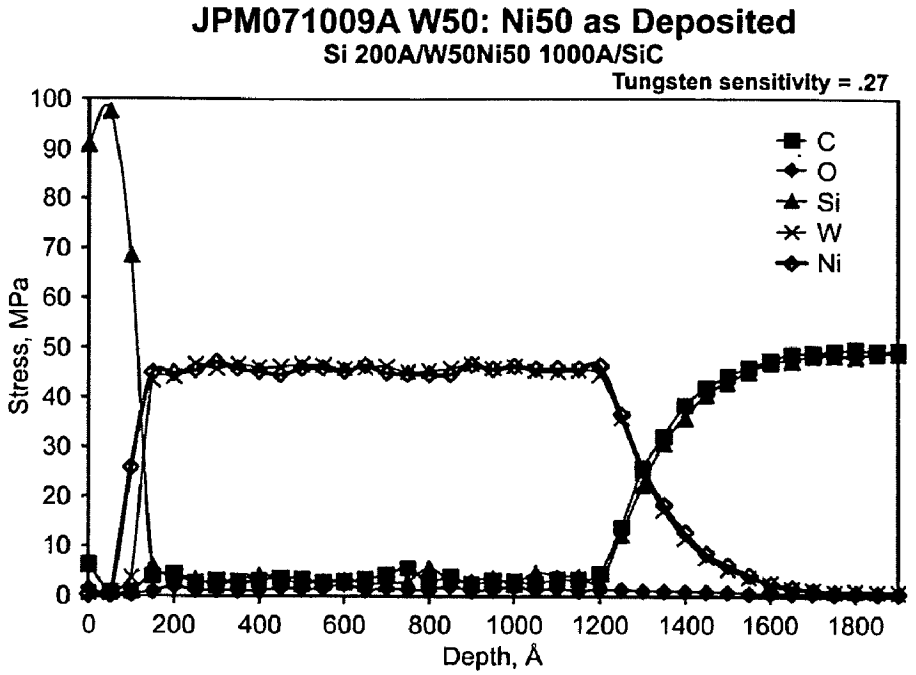
JPM071009A W50: Ni50 as Deposited
Si 200A/W50Ni50 1000A/SiC
Tungsten sensitivity = .27
C
O
Si
W
Ni
Stress, MPa
100
90
80
70
60
50
40
30
20
10
0
0
200
400
600
800
1000
1200
1400
1600
1800
Depth, Å

Figure 9

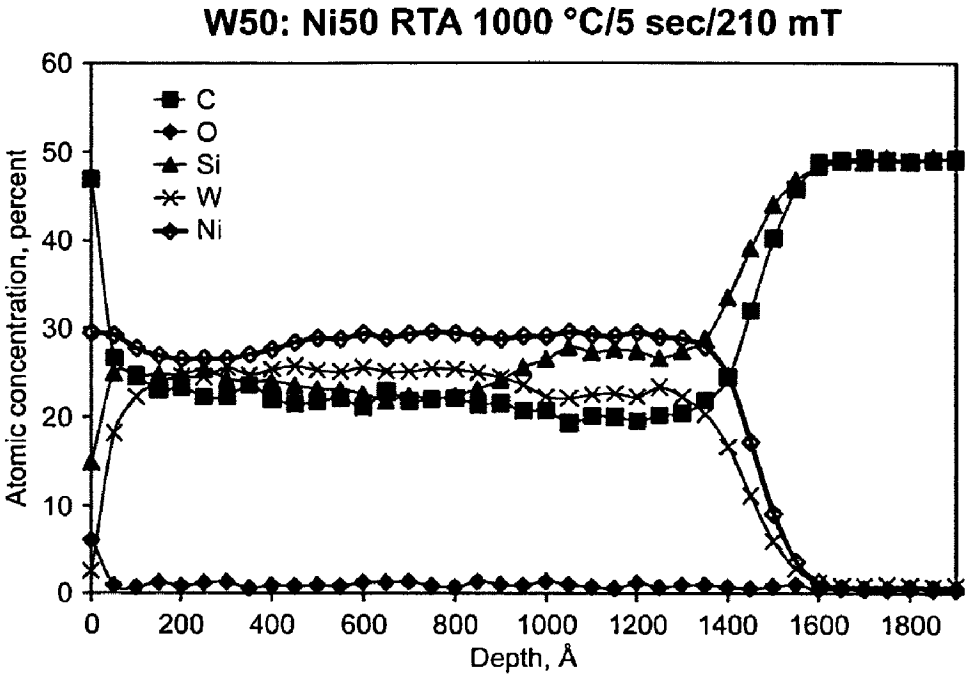
W50: Ni50 RTA 1000 °C/5 sec/210 mT
Atomic concentration, percent
Depth, Å
C
O
Si
W
Ni
0
10
20
30
40
50
60
0
200
400
600
800
1000
1200
1400
1600
1800

Figure 10

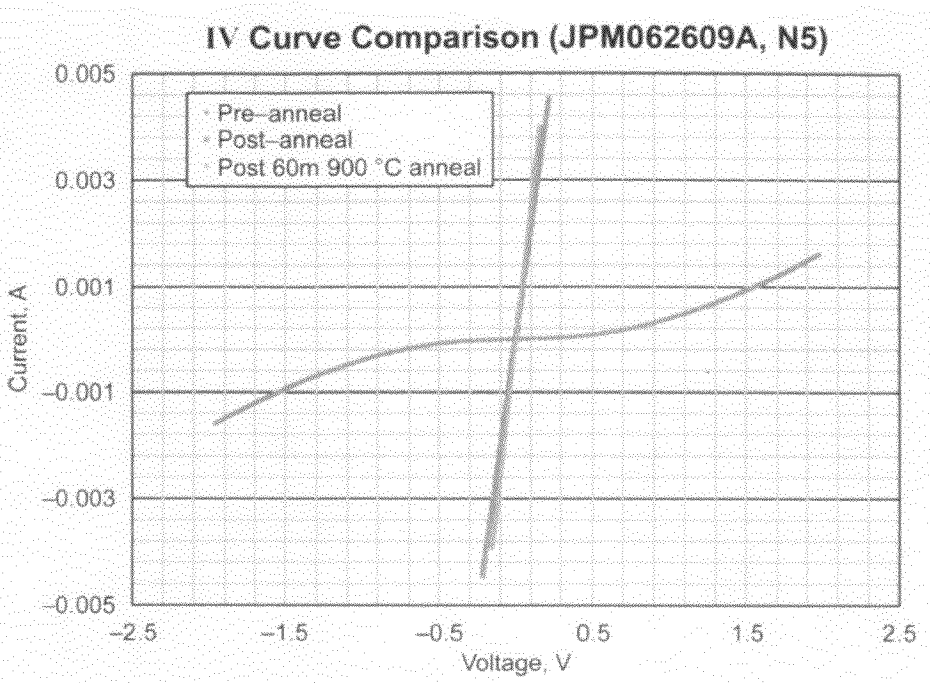


Table A

| Annealing conditions | |
|---|---|
| Time | 5 s |
| Temperature | 1000 °C |
| Pressure | 239 mTorr |
| Gas backfill | None |

Table B

| | |
|---|---|
| Doping level | $>2\times10^{19}$ (n-type) |
| Metal deposited | W75–Ni25 1000 Å |
| | Si (200 Å) cap |

Figure 11

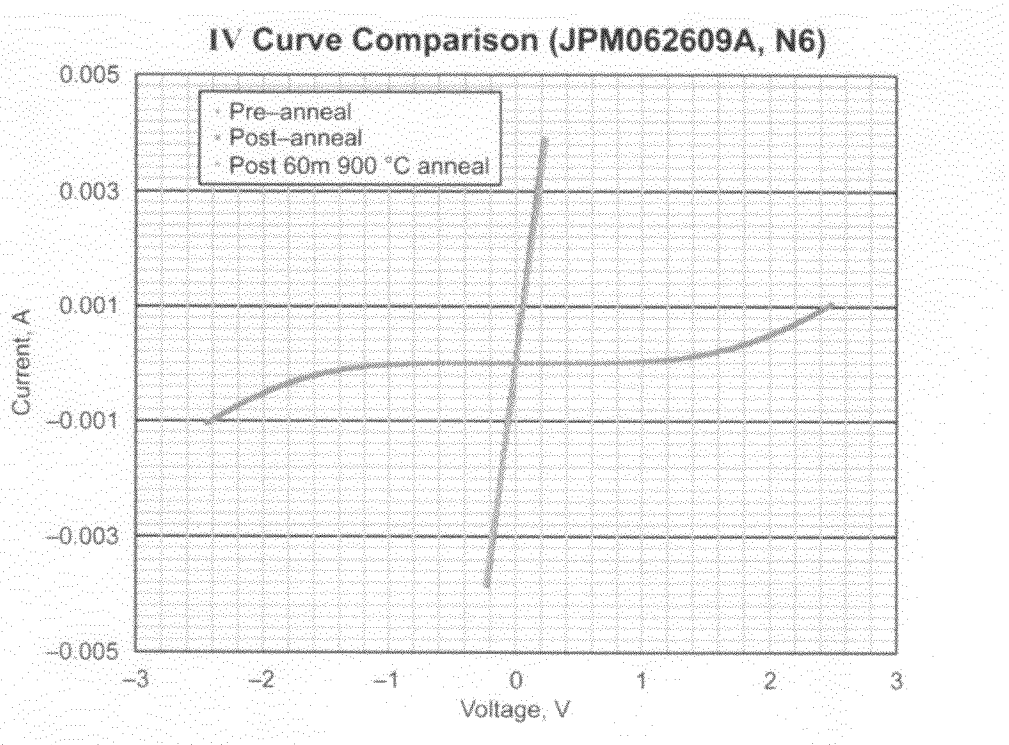


Table A

| Annealing conditions | |
|---|---|
| Time | 5s |
| Temperature | 1000 °C |
| Pressure | 239 mTorr |
| Gas backfill | None |

Table B

| | |
|---|---|
| Doping level | $1.4\times10^{19}$ (n-type) |
| Metal deposited | W75–Ni25 (1000 Å) |
| | Si (200 Å) cap |

Figure 12

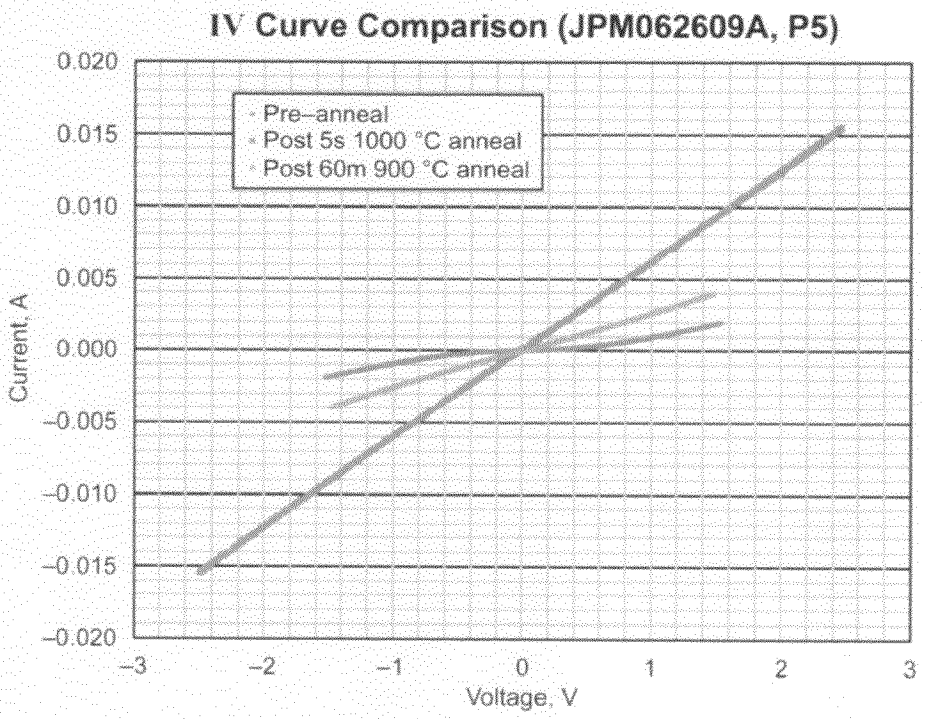


Table A

| Annealing conditions | |
|---|---|
| Time | 5 s |
| Temperature | 1000 °C |
| Pressure | 239 mTorr |
| Gas backfill | None |

Table B

| | |
|---|---|
| Doping level | $>2\times10^{19}$ (p-type) |
| Metal deposited | W75–Ni25 (1000 Å) Si (200 Å) cap |

Figure 13

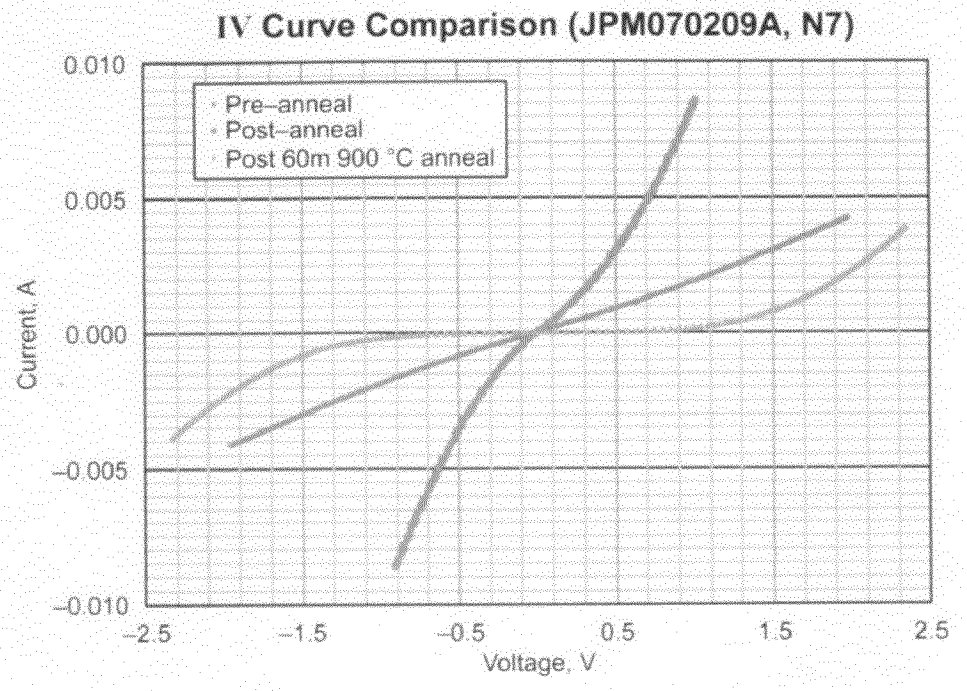


Table A

| Annealing conditions | |
|---|---|
| Time | 5 s |
| Temperature | 1000 °C |
| Pressure | 239 mTorr |
| Gas backfill | None |

Table B

| | |
|---|---|
| Doping level | $>2\times10^{19}$ (n-type) |
| Metal deposited | W90–Ni10 (1000 Å) Si (200 Å) cap |

Figure 14

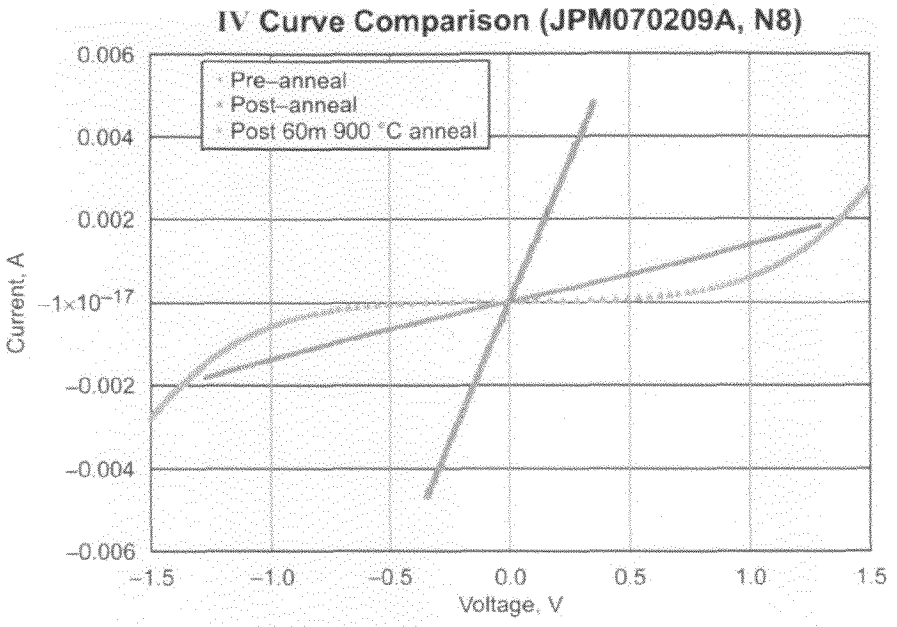


Table A

| Annealing conditions | |
|---|---|
| Time | 5 s |
| Temperature | 1000 °C |
| Pressure | 239 mTorr |
| Gas backfill | None |

Table B

| | |
|---|---|
| Doping level | $1.4\times10^{19}$ (n-type) |
| Metal deposited | W90–Ni10 (1000 Å) |
| | Si (200 Å) cap |

Figure 15

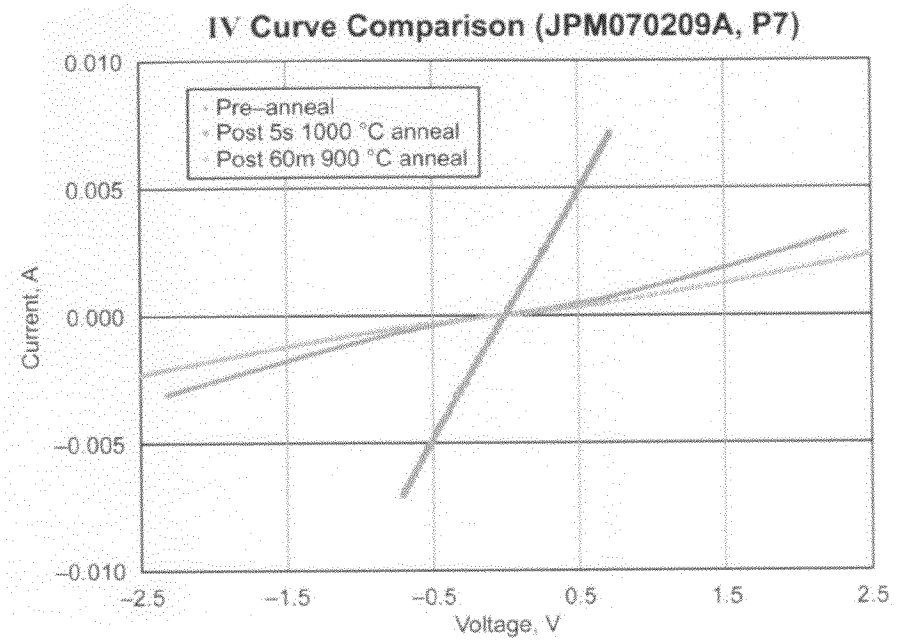


Table A

| Annealing conditions | |
|---|---|
| Time | 5 s |
| Temperature | 1000 °C |
| Pressure | 239 mTorr |
| Gas backfill | None |

Table B

| | |
|---|---|
| Doping level | $>2\times10^{19}$ (p-type) |
| Metal deposited | W90–Ni10 (1000 Å) |
| | Si (200 Å) cap |

Figure 16

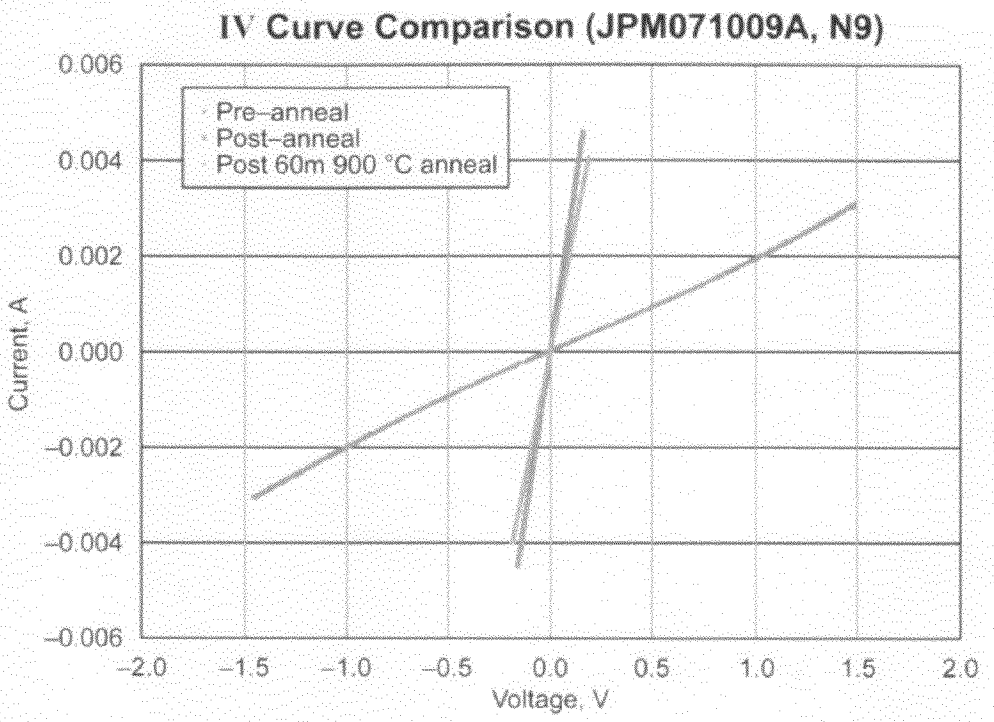


Table A

| Annealing conditions | |
|---|---|
| Time | 5 s |
| Temperature | 1000 °C |
| Pressure | 239 mTorr |
| Gas backfill | None |

Table B

| | |
|---|---|
| Doping level | $>2\times10^{19}$ (n-type) |
| Metal deposited | W50–Ni50 (1000 Å) Si (200 Å) cap |

Figure 17

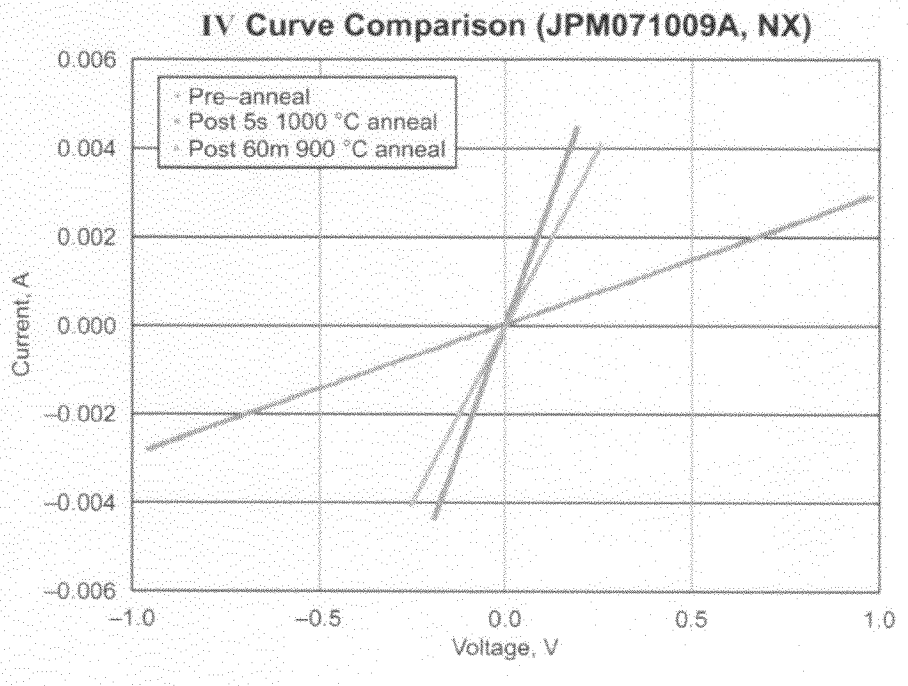


Table A

| Annealing conditions | |
|---|---|
| Time | 5 s |
| Temperature | 1000 °C |
| Pressure | 239 mTorr |
| Gas backfill | None |

Table B

| | |
|---|---|
| Doping level | $1.4\times10^{19}$ (n-type) |
| Metal deposited | W50–Ni50 (1000 Å) Si (200 Å) cap |

Figure 18

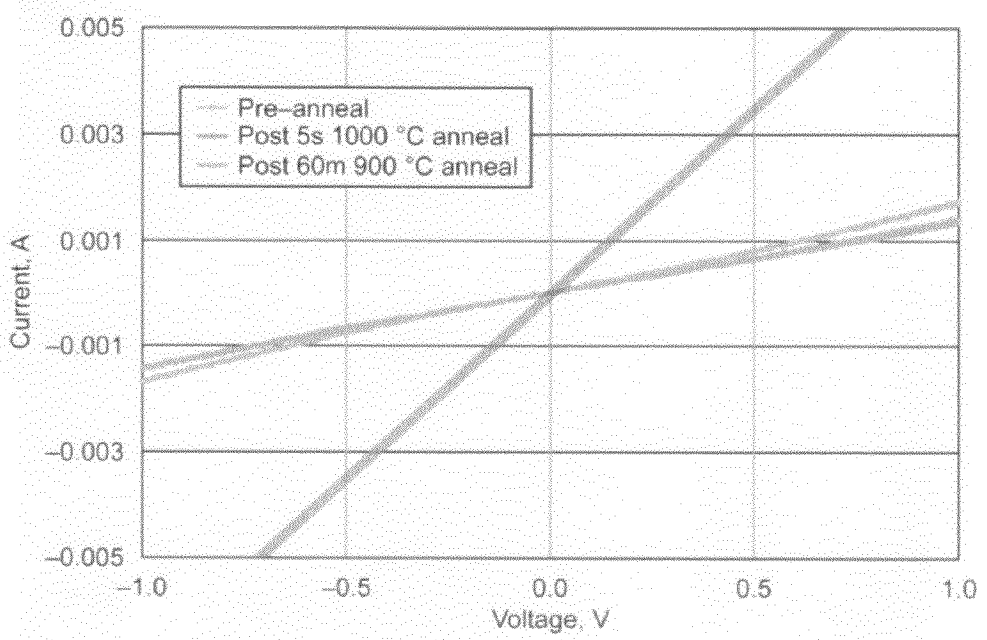


Table A

| Annealing conditions | |
|---|---|
| Time | 5 s |
| Temperature | 1000 °C |
| Pressure | 239 mTorr |
| Gas backfill | None |

Table B

| | |
|---|---|
| Doping level | $>2\times10^{19}$ (p-type) |
| Metal deposited | W50–Ni50 (1000 Å) |
| | Si (200 Å) cap |

Figure 19

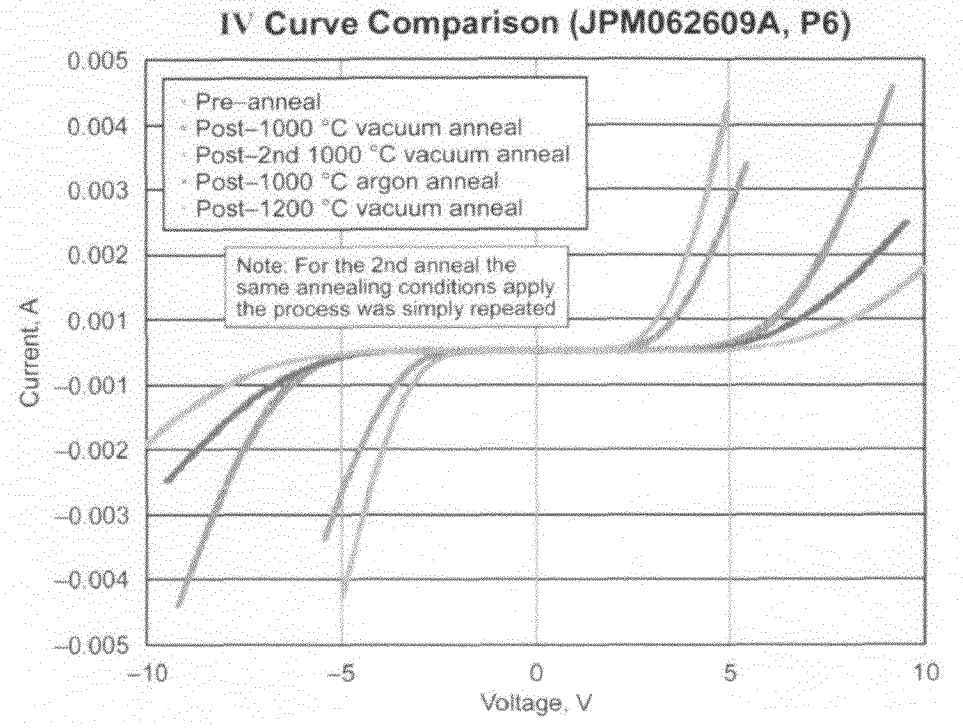


Table A

| Annealing conditions | |
|---|---|
| Time | 5 s |
| Temperature | 1000 °C |
| Pressure | 239 mTorr |
| Gas backfill | None |

Table B

| | |
|---|---|
| Doping level | $1.6\times10^{19}$ (p-type) |
| Metal deposited | W75–Ni25 (1000 Å) |
| | Si (200 Å) cap |

Figure 20

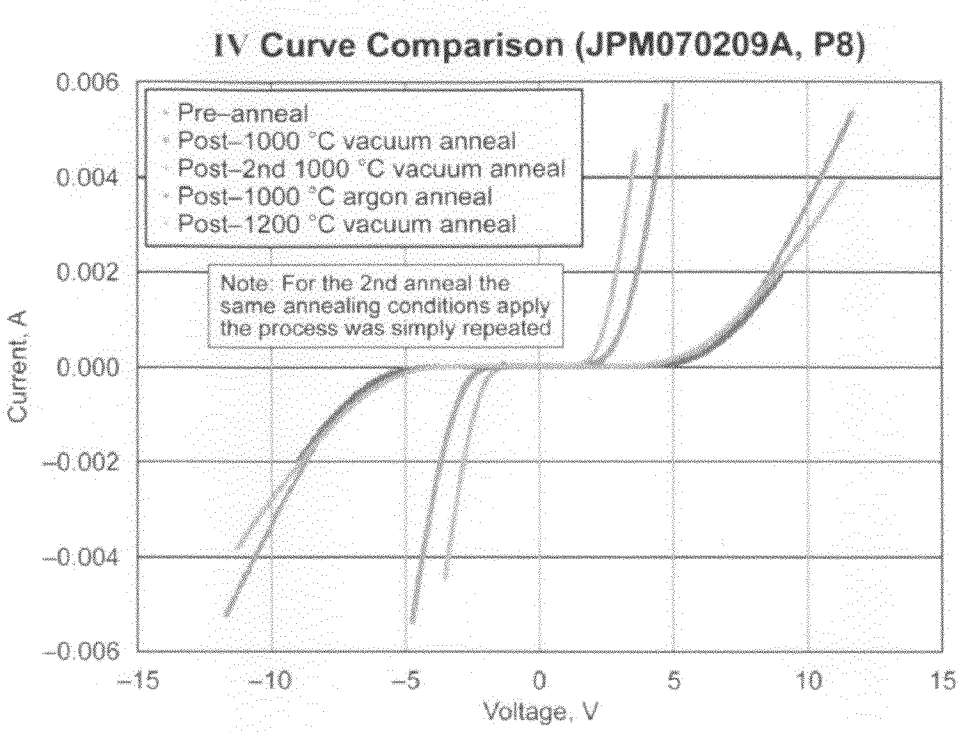


Table A

| Annealing conditions | |
|---|---|
| Time | 5 s |
| Temperature | 1000 °C |
| Pressure | 239 mTorr |
| Gas backfill | None |

Table B

| | |
|---|---|
| Doping level | $1.6\times10^{19}$ (p-type) |
| Metal deposited | W90–Ni10 (1000 Å) Si (200 Å) cap |

Figure 21

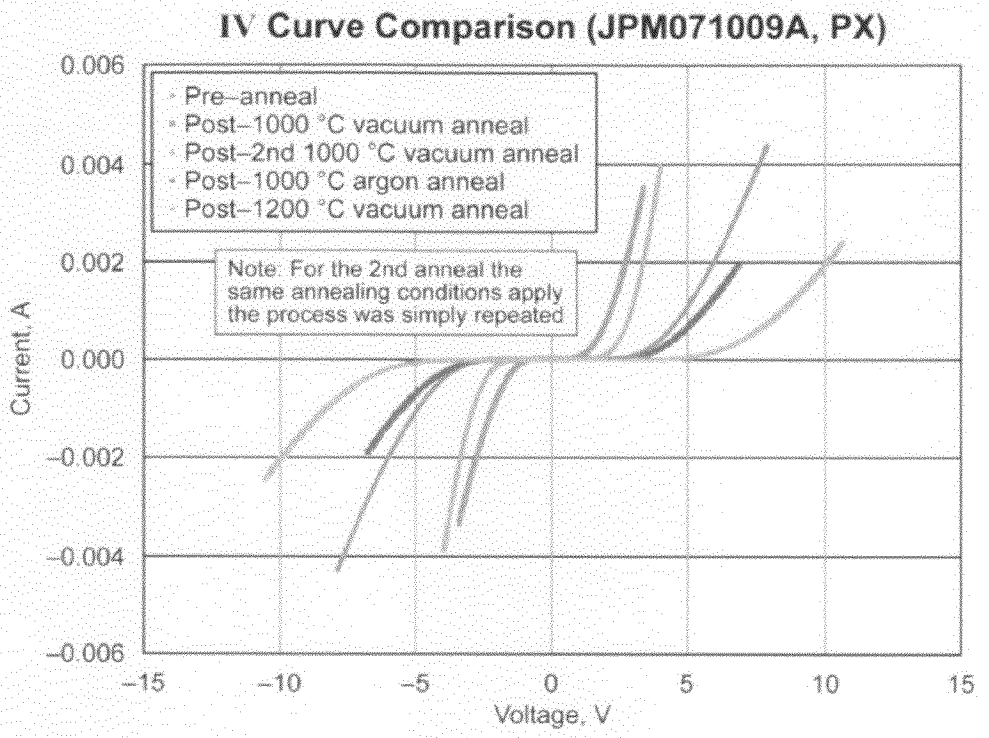


Table A

| Annealing conditions | |
|---|---|
| Time | 5 s |
| Temperature | 1000 °C |
| Pressure | 239 mTorr |
| Gas backfill | None |

Table B

| | |
|---|---|
| Doping level | $1.6\times10^{19}$ (p-type) |
| Metal deposited | W50–Ni50 (1000 Å) Si (200 Å) cap |

Figure 22

TABLE 3[a]

| | Pre-anneal | | |
|---|---|---|---|
| Doping level | W90–Ni10 | W75–Ni25 | W50–Ni50 |
| $>2\times10^{19}$ n-type | Ohmic | Rectifying | Ohmic |
| $1.4\times10^{19}$ n-type | Ohmic | Rectifying | Ohmic |
| $>2\times10^{19}$ p-type | Ohmic | Rectifying | Ohmic |
| $1.6\times10^{19}$ p-type | Rectifying | Rectifying | Rectifying |

| | Post 5 s 1000 °C anneal | | |
|---|---|---|---|
| Doping level | W90–Ni10 | W75–Ni25 | W50–Ni50 |
| $>2\times10^{19}$ n-type | Ohmic | Ohmic | Ohmic |
| $1.4\times10^{19}$ n-type | Ohmic | Ohmic | Ohmic |
| $>2\times10^{19}$ p-type | Ohmic | Ohmic | Ohmic |
| $1.6\times10^{19}$ p-type | Rectifying | Rectifying | Rectifying |

| | Post 60 min 900 °C anneal | | |
|---|---|---|---|
| Doping level | W90–Ni10 | W75–Ni25 | W50–Ni50 |
| $>2\times10^{19}$ n-type | Rectifying | Ohmic | Ohmic |
| $1.4\times10^{19}$ n-type | Rectifying | Ohmic | Ohmic |
| $>2\times10^{19}$ p-type | Ohmic | Ohmic | Ohmic |
| $1.6\times10^{19}$ p-type | Rectifying | Rectifying | Rectifying |

[a]For our tests an IV curve is ohmic if it has an $R^2$ value of greater than 0.99.

**Figure 23**

TABLE OF WORK FUNCTION OF METAL SILICIDES AND CARBIDES

| Carbides | Work function | Silicides | Work function |
|---|---|---|---|
| Al | | x | |
| TiC | 3.8/4.1 | $Ti_5Si_3$ | 3.7 (n-type) |
| | | TiSi | 3.9 (n-type) |
| | | $TiSi_2$ | 3.95 to 4.18 (n-type) |
| VC | 4.3 | $VSi_2$ | 4.63 |
| $Cr_3C_2$ | 5.10 to 5.20 (p-type) | $CrSi_2$ | 4.32 |
| Mn | x | Mn | |
| Co | x | $Co_2Si$ | 4.87 |
| | | CoSi | 4.55 |
| | | $CoSi_2$ | 4.56 |
| Ni | x | $Ni_2Si$ | 4.79 (n-type) |
| | | NiSi | 4.93 (n-type) |
| | | $NiSi_2$ | 4.54 (n-type) |
| Cu | x | Cu | |
| Se | | Se on Si | 5.9 |
| Pd | x | $Pd_2Si$ | 5.04 (p-type) |
| Rh | | Rh on SiO2 | 5.43 |
| Ru | | Ru | 4.71 |
| $Mo_2C$ | 3.5 to 3.8 | $MoSi_2$ | 4.9 |
| NbC | 4.1 | $NbSi_2$ | 4.3 |
| ZrC | 3.70 | | |
| HfC | 4.63 | | |
| TaC | 4.38 | $TaSi_2$ | 4.71 |
| $TaC_xN_y$ | 4.6 to 5.2 | | |
| WC-C | 6.3 (p-type) | $W_5Si_3$ | 4.31 |
| WC-W | 5.3 (p-type) | $WSi_2$-Si | 4.76 (n-type) |
| | | $WSi_2$-W | 5.1 (p-type) |
| Re | | Re | |
| Os | | $OsSi_{1.8}$ | 4.75 |
| Ir | | IrSi | 5.08 |
| Pt | x | PtSi, $Pt_2Si$ | 5.15 to 5.75 (p-type) |

Figure 24

# DUAL OHMIC CONTACT TO N- AND P-TYPE SILICON CARBIDE

## ORIGIN OF THE INVENTION

The invention described herein was made by an employee of the United States Government and may be manufactured and used only by or for the Government for Government purposes without the payment of any royalties thereon or therefore.

## BACKGROUND

Traditional high temperature devices are generally placed several distances from high temperature environments in order to prevent them from failing, due to the inability to survive the high temperature. Generally, the failure of these devices (e.g., sensors and electronics) is due to the instability or lack of robustness of the contact metallization and packaging. Unique problem characteristics are the effects posed by temperature on semiconductor sensors and electronics as they are further inserted into the higher temperature sections of the monitored environment. This is primarily because, as the devices with traditional electrical ohmic contacts are inserted further into higher temperature sections, their performance characteristics degrade dramatically to the point that they fail catastrophically.

As a result of the aforementioned scenario, devices with conventional ohmic contact metallization are generally placed several distances away from environments having extreme temperatures. In other words, the devices are positioned in lower temperature sections (e.g., of an engine) where the temperature would not adversely impact the contact metallization or the package.

In addition to the above disadvantage of conventional metallization on devices, there is also a problem of complexity and production costs that is associated with their fabrication. Most semiconductor electronic and some sensing devices operate in bi-polar mode, which means that the device's physical configuration contains sections that are doped either n- or p-type. As a result, the metallization needed to make ohmic contact to either of the layers is exclusive to that layer. This means that below a certain doping level, a metal (or metal compound/mixture) that is ohmic on an n-doped layer generally would be rectifying on a p-doped layer. Conversely, a metallization that is ohmic on a p-doped layer would be rectifying if deposited on an n-doped layer.

Therefore, on a bi-polar device, multiple process steps of successive depositions, photolithography, and etchings are required to deposit and pattern the desired ohmic contact metallization. This process is time consuming and expensive. For example, in some instances, one of the layers is degenerately doped (usually the p-type SiC) so that the exclusivity is removed, thereby making it possible for a single metal to be ohmic on both n- and p-type layers. The process of forming a degenerately doped layer in the contact area is by high-energy ion implantation. This entails surface preparation prior to ion implantation, usually performed at temperatures around 1100° C. As can be appreciated, the process not only adds cost, but the implantation process itself causes damage to the lattice structure of the device. The induced damage can only be partially reversed after annealing. Post ion implantation also requires that the implant be activated at temperature as high as 1200° C., and it is known that not all the implants are fully activated.

## SUMMARY

The following presents a simplified summary in order to provide a basic understanding of some aspects of the innovation. This summary is not an extensive overview of the innovation. It is not intended to identify key/critical elements or to delineate the scope of the innovation. Its sole purpose is to present some concepts of the innovation in a simplified form as a prelude to the more detailed description that is presented later.

The innovation disclosed and claimed herein, in one aspect thereof, comprises a simultaneous formation of electrical ohmic contacts to silicon carbide (SiC) semiconductor having donor and acceptor impurities (n- and p-type doping, respectively). More particularly, the ohmic contact can be formed on SiC layers having n- and p-type doping at one process step during the fabrication of the semiconductor device. Accordingly, the multiple process steps for fabricating contacts on to n- and p-type surfaces can be greatly reduced, thereby reducing time and cost, and increasing yield.

Additionally, the innovation discloses a metallization scheme that can serve as a non-discriminatory, universal ohmic contact to both n- and p-type SiC, without compromising the reliability of the specific contact resistivity when operated at temperatures in excess of 600° C.

To the accomplishment of the foregoing and related ends, certain illustrative aspects of the innovation are described herein in connection with the following description and the annexed drawings. These aspects are indicative, however, of but a few of the various ways in which the principles of the innovation can be employed and the subject innovation is intended to include all such aspects and their equivalents. Other advantages and novel features of the innovation will become apparent from the following detailed description of the innovation when considered in conjunction with the drawings.

## BRIEF DESCRIPTION OF THE DRAWINGS

FIG. **1** illustrates example specifications of a Tungsten (W) uniformity experiment in accordance with the innovation.

FIG. **2** illustrates example results of a W uniformity experiment in accordance with the innovation.

FIG. **3** illustrates an example Silicon (Si) uniformity experiment in accordance with aspects of the innovation.

FIG. **4** illustrates example results of a Si uniformity experiment in accordance with the innovation.

FIG. **5** illustrates an example Auger Electron Spectroscopy graph in accordance with a Si uniformity experiment in accordance with the innovation.

FIG. **6** illustrates an example photograph of a W/Si annealing experiment in accordance with the innovation.

FIG. **7** illustrates example stress results in accordance with an aspect of the innovation.

FIG. **8** illustrates example stress results in accordance with an aspect of the innovation.

FIG. **9** illustrates example Auger data in accordance with an aspect of the innovation.

FIG. **10** illustrates example results following annealing in accordance with an aspect of the innovation.

FIGS. **11-19** illustrate example comparative graphs for each sample (N**5**, N**6**, N**7**, N**8**, N**9**, NX, P**5**, P**7** and P**95**) and their three different measurements in accordance with aspects of the innovation.

FIG. **20** illustrates example results from sample P**6** after several annealing attempts in accordance with aspects of the innovation.

FIG. **21** illustrates example results from sample P**8** after several annealing attempts in accordance with aspects of the innovation.

FIG. **22** illustrates example results from sample PX after several annealing attempts in accordance with aspects of the innovation.

FIG. **23** illustrates an example summary chart of a WNi scheme in accordance with aspects of the innovation.

FIG. **24** illustrates an example work function table of metal silicides and carbides in accordance with aspects of the innovation.

## DETAILED DESCRIPTION

The following terms are used throughout the description, the definitions of which are provided herein are included to assist in understanding various aspects of the subject innovation. The definitions are not intended to limit the scope of this specification in any manner.

Chemical etching refers to a process of using acids, bases or other chemicals to dissolve unwanted materials such as metals or semiconductor materials;

Current-Voltage Characteristic (I-V Curve) refers to a relationship, typically represented as a chart or graph, in which an electric current is measured as function of voltage;

Electron beam evaporation refers to a process of deposition in which an electron beam is directed at a crucible of metal. The electron beam causes atoms from the target to transform into the gaseous phase. These atoms then precipitate into solid form coating everything in the vacuum chamber with a thin layer of the material;

Glow discharge refers to a conduction of electricity in a low-pressure gas, producing a diffuse glow;

Photoelectron spectroscopy refers to energy measurement of electrons emitted from solids, gases or liquids by the photoelectric effect, in order to determine the binding energies of electrons in a substance. There are two types described infra, Auger Photoelectron Spectroscopy and X-Ray Photoelectron Spectroscopy (XPS);

Physical vapor deposition refers to a general term used to describe most any of a variety of methods to deposit thin films by the condensation of a vaporized form of the material onto various surfaces;

Probe station is used to acquire signals from the internal nodes of a semiconductor device. In the following discussion, a probe station is used to measure I-V Curves;

Rapid Thermal Anneal (RTA) refers to a semiconductor manufacturing process that heats a substrate and the thin film on it to high temperatures in several seconds or less. During cooling, wafer temperatures are decreased slowly in order to prevent the breaking of the substrate;

Scanning Electron Microscope (SEM) refers to a type of electron microscope that images a sample surface by scanning it with a high-energy beam of electrons in a raster scan pattern;

Semiconductor is a material that has an electrical resistivity between that of a conductor and an insulator. Semiconductor properties are often affected by the environment they are in, e.g., in a high temperature environment a semiconductor's resistivity will generally be lower;

Sputtering refers to a process that uses ions of an inert gas to dislodge atoms from the surface of a crystalline material, the atoms then being electrically deposited to form an extremely thin coating on a glass, metal, plastic, or other surface;

Substrate refers to a supporting material on which a circuit is formed or fabricated, e.g., where the atoms from the target are collected as a thin film;

Target refers to a circular object made of the material that is to be sputtered; and

Work function refers to the minimum amount of energy required to remove an electron from the surface of a metal.

The innovation is now described with reference to the drawings, wherein like reference numerals are used to refer to like elements throughout. In the following description, for purposes of explanation, numerous specific details are set forth in order to provide a thorough understanding of the subject innovation. It may be evident, however, that the innovation can be practiced without these specific details.

Wide-bandgap materials generally offer nearly ideal properties for fast, hot, high-power electronics. They have attractive properties but have high melting points that are greater than that of silicon and gallium arsenide, and they have taken the semiconductor industry the longest to understand and produce commercially. They have benefitted from much of the development in silicon electronics, but silicon-based products are much less expensive to manufacture. Therefore, wide-bandgap electronics have to compete in those niches where silicon and other solutions are inferior.

The innovation discloses a dual ohmic contact metallization scheme that can enhance the performance of semiconductor SiC sensors and electronics for the purpose of improved safety, efficient operation, and reduction of costs associated with premature equipment down time, future aero-engines, manufacturing processes, and environmental monitoring. These applications are commonly characterized by temperatures greater than 600° C. which require more proximal insertion of sensors and electronics. For example, combustion chambers of jet engines and rocket engines operate at temperatures at and above 1000° C. The proximal insertion of these devices in the high temperature sections could provide real time monitoring of changes that are occurring, thereby allowing for a faster decision making process to mitigate events that are predetermined to be undesirable and could lead to a catastrophic result if not sufficiently controlled.

The innovation discloses generation and implementation of a simultaneous electrical ohmic contact to n- and p-type silicon carbide (SiC) semiconductor material. In accordance with aspects, such ohmic contact metallization can be thermally stable at extreme temperatures, e.g., beyond 600° C. The supporting theory is based on the use of a combination of material work functions as a basis for non-discriminatory charge transport across the metallurgical junction of the metal and the semiconductor.

Generally, in the absence of Fermi level pinning, ohmic contact formation is favored when a metal or metal compound having a work function that is lower than the work function (or electron affinity) of the n-doped (donor-type) semiconductor is deposited on such semiconductor. However, when such metal or metal compound is deposited on the p-doped (acceptor-type) semiconductor with a greater work function, a rectification occurs. Conversely, a metal or metal compound with a work function greater than the work function of a p-doped semiconductor favors an ohmic contact formation, but would rectify on the n-doped layer. It will be understood that a "work function" refers to the minimum energy (e.g., electron volts) needed to remove an electron from a solid to a point immediately outside the solid surface. In other words, a "work function" can refer to the energy required to move an electron from the Fermi level into vacuum.

Based on the above brief theoretical description of metal-semiconductor charge transport on which this innovation is based, it is desired to simultaneously form ohmic contact on both n-type and p-type SiC. By a careful selection of the appropriate combination of metal carbides/silicides with work functions greater than the work function of p-type SiC and another combination metal carbides/silicides with work

functions less than the work function of n-type SiC, and then mixing both combination together, simultaneous ohmic contacts on both n- and p-type surfaces can be favored.

Work functions of metal carbides and silicides can be employed to identify materials that theoretically support the concept of simultaneous forming ohmic contact on both n- and p-type SiC. One such combination of metals that was selected for the proof of concept is a mixture of Tungsten (W) and Nickel (Ni), which when annealed (i.e., heated) on SiC would form metal compounds of tungsten carbide, tungsten silicide, and nickel silicide. It is stated in the literature that the work function of tungsten carbide ranges between 5 and 6.3 eV while the work function of tungsten silicide varies from 4.3 to 5.2 eV. The work function of nickel silicide is between 4.5 and 4.93 eV.

As a further observation, tungsten silicide is being observed alongside tungsten carbide and nickel silicide as reaction products. The presence of high tungsten silicide is being observed at the silicon carbide interface, which could be playing a significant role in the formation of the dual ohmic contact.

While WNi aspects are described in detail, it is to be understood that other metal silicides and carbides can be employed in alternative aspects of the innovation. FIG. **25** illustrates an example table of metal silicides and carbides having work functions that may satisfy the work function characteristics and rules as described herein. These example metal silicides and carbides are to be included within the scope of this disclosure and claims appended hereto.

For n-type SiC, the work function is about 4.75 eV while the work function of p-type SiC is about 4.85 eV. Therefore, ohmic contact is favored when variations of nickel silicide with work functions less than that of n-type SiC are used. On the other hand, ohmic contact on p-type SiC is favored when the work functions of variations of tungsten carbide is greater than that of the p-type SiC. The above theory was validated and reproduced by using a combination of tungsten and nickel as described in greater detail.

As illustrated and described in detail infra, test data confirms that simultaneous ohmic contact can be formed on n-type and p-type 4H—SiC. For the n-type, ohmic contact was demonstrated for doping level starting from $1.4\times10^{19}$ $cm^{-3}$ and higher. For the p-type, ohmic contact was demonstrated for doping levels greater than $2\times10^{19}$ $cm^{-3}$. It will be appreciated that lower doping levels can be employed in alternative aspects.

The following discussion performs a characterization of selected thin films for the purpose of developing enhanced electrical contacts (ohmic contacts) to SiC. The discussion references characteristics of different materials in order to suggest which ones would be suitable for the desired solution. These characterizations include deposition uniformity, deposition rate, film composition, stress analysis, electrical analysis (pre- & post RTA), and several other analytical processes. It will be appreciated that these characteristics are important in creating a stable contact. Using this information, development can begin regarding the metallization that can establish an enhanced ohmic contact that can survive and be stable at temperatures of about 1000° C.

The innovation can be used to develop a new ohmic contact metallization that would enable semiconductor functionality at about 1000° C. Essentially, as will be understood upon a review of the discussion that follows, the innovation can characterize a new high temperature metallization scheme, demonstrate ohmic contact to n- and p-type SiC, and demonstrate a thermally stable ohmic contact to SiC. The findings can be implemented into enhanced devices such as sensors or the like.

W—Ni Experiments (Patterning, Annealing, & Electrical Analysis)

In order to test the metallization electrical characteristics, several processes were performed. The tests employed three different WNi compositions, $W_{90}Ni_{10}$, $W_{75}Ni_{25}$, and $W_{50}Ni_{50}$. They would be tested using four samples each with different doping levels. $W_{75}Ni_{25}$ would be done first and its samples would be labeled N**5**, N**6**, P**5**, and P**6**. $W_{90}Ni_{10}$ would be done second and its samples would be labeled N**7**, N**8**, P**7**, and P**8**. $W_{50}Ni_{50}$ would be done third and its samples would be labeled N**9**, NX, P**9**, and PX.

The odd-numbered n-type samples were of the doping level $>2\times10^{19}$ $cm^{-3}$. The even-numbered n-type samples were of the doping level $1.4\times10^{19}$ $cm^{-3}$. The odd-numbered p-type samples were of the doping level $>2\times10^{19}$ $cm^{-3}$. And the even-numbered p-type samples were of the doping level $1.6\times10^{19}$ $cm^{-3}$. The steps in the process would include Photolithography with photoresist (PR), Aluminum (Al) deposition, Al/PR liftoff, WNi deposition, and WNi/Al liftoff. After performing all of these steps, next is to test the initial (pre-annealed) contact. Thereafter, each sample was diced into quarters and select quarters underwent an annealing process after which they were again tested electrically. The photolithography process was completed using the deep reactive ion etching test mask and AZ5214E photoresist.

After the PR was patterned, using the Telemark E-Beam, 5000 Å of Al were deposited onto each sample. Immediately following the cool down, the samples were unloaded and placed in an Acetone and Isopropanol bath to liftoff the PR and the Al deposited on top of it to reveal the reversed image of the desired pattern.

The samples were then placed into a two chamber Lesker sputtering system and received 1000 Å of WNi according to which composition they were assigned. Each sample was given a 200 Å Si Cap. After the deposition and the appropriate cool down time, the samples were placed in a bath of hot phosphoric acid at 50° C. This process lifts off the Al and the WNi/Si on top to leave the desired test pattern of WNi/Si. After liftoff the samples were evaluated by taking I-V characteristic measurements. Thereafter, a layer of PR was placed on each sample to protect the surface during dicing.

The samples were taken and diced into quarters at which point one quarter of each sample was annealed at 1000° C. for 5 sec under vacuum with a pressure of 239 mTorr, after which I-V characteristic measurements were again taken. After these measurements were taken and compared, the samples that displayed an ohmic contact (N**5**, N**6**, N**7**, N**8**, N**9**, NX, P**5**, P**7**, P**9**) went back into the RTA for an aging process to test the durability of each sample. They were annealed for 60 minutes at 900° C. under Ar with a flow rate of twice the normal rate. After each of these steps, the samples were taken and analyzed. The comparative graphs for each sample (N**5**, N**6**, N**7**, N**8**, N**9**, NX, P**5**, P**7**, P**9**) and their three different measurements are displayed in the results section of FIGS. **11**, **12**, **13**, **14**, **15**, **16**, **17**, **18**, and **19** respectively.

Re-Annealing Experiment

When viewing the results of the anneal and realizing that the lowest doped p-type samples were not ohmic, it was decided to do the same annealing run again on those three samples (P**6**, P**8**, & PX) to determine if perhaps the reaction was not complete yet and if 5 more seconds would positively alter the results. For P**6** and P**8** the cut in voltage was decreased slightly after re-annealing. However for PX the re-anneal only hindered the contact.

Argon Annealing Experiment

After reviewing the results of the initial annealing test, one quarter from P6, P8, and PX were then annealed for 5 seconds at 1000° C. under Ar. This was done to attempt to make an ohmic contact to the lower doped p-type sample that in the last test was not ohmic. This proved to be an unfruitful experiment, as the electrical tests revealed that after annealing with Ar, not even the cut in voltage on the rectifying curve was decreased.

1200° C. Annealing Experiment

After reviewing the results of the Argon anneal, it was decided to again take a sample from P6, P8, and PX and anneal at 1200° C. for 5 sec under vacuum. This was done at a pressure of 239 mTorr. This was also not a fruitful experiment other than realizing that neither annealing in Ar or at 1200° C. in vacuum will aid in making the lower doped p-type samples ohmic. Graphs comparing the results as deposited, initial anneal, re-anneal, Ar anneal, & 1200° C. anneal electrical measurements are displayed in the results section of FIGS. **20**, **21** and **22**.

N5 (FIG. **11**) was doped at $>2\times10^{19}$ $cm^{-3}$ n-type and has $W_{50}Ni_{50}$ (1000 Å) and a Si cap (200 Å). It was first annealed for 5 seconds at 1000° C. and then for 60 minutes at 900° C. N6 (FIG. **12**) was doped at $1.4\times10^{19}$ $cm^{-3}$ n-type and has $W_{50}Ni_{50}$ (1000 Å) and a Si cap (200 Å). It was first annealed for 5 seconds at 1000° C. and then for 60 minutes at 900° C. Both n-type samples from the $W_{75}Ni_{25}$ composition turned out to be ohmic only after annealing but showed signs of stability after 60 min at 900° C.

P5 (FIG. **13**) was doped at $>2\times10^{19}$ $cm^{-3}$ p-type and has $W_{50}Ni_{50}$ (1000 Å) and a Si cap (200 Å). It was first annealed for 5 seconds at 1000° C. and then for 60 minutes at 900° C. N7 (FIG. **14**) was doped at $>2\times10^{19}$ $cm^{-3}$ n-type and has $W_{90}Ni_{10}$ (1000 Å) and a Si cap (200 Å). It was first annealed for 5 seconds at 1000° C. and then for 60 minutes at 900° C. The p-type sample although ohmic after the first anneal increased in resistance after the second anneal. The n-sample for $W_{90}Ni_{10}$ lost its ohmic contact completely.

N8 (FIG. **15**) was doped at $1.4\times10^{19}$ $cm^{-3}$ n-type and P7 (FIG. **14**) was doped at $>2\times10^{19}$ $cm^{-3}$ p-type. They both have $W_{90}Ni_{10}$ (1000 Å) and a Si cap (200 Å). It was first annealed for 5 seconds at 1000° C. and then for 60 minutes at 900° C. N8 shows similar results to N7 in that it was initially going ohmic but after 60 minutes at 900° C. the contact became rectifying. P7 however retained its ohmic contact but only slightly. In all three $W_{90}Ni_{10}$ cases the resistance began to rise during the 60 minute Anneal at 900° C.

N9 (FIG. **17**) was doped at $>2\times10^{19}$ $cm^{-3}$ n-type and NX (FIG. **18**) was doped at $1.4\times10^{19}$ $cm^{-3}$ n-type. They both have $W_{50}Ni_{50}$ (1000 Å) and a Si cap (200 Å). It was first annealed for 5 seconds at 1000° C. and then for 60 minutes at 900° C. Both N9 and NX decreased significantly in resistance after the first anneal. However, after 60 minutes at 900° C. the contact appeared to begin to gain resistivity. Although in comparison to other metallizations, $W_{50}Ni_{50}$ changed the least after the second anneal/aging process.

P9 (FIG. **19**) was doped at $>2\times10^{19}$ $cm^{-3}$ p-type and has a film containing $W_{50}Ni_{50}$ (1000 Å) and a Si cap (200 Å). It was first annealed for 5 seconds at 1000° C. and then for 60 minutes at 900° C. While remaining ohmic throughout all steps, the resistance values decreased significantly after the first anneal and then increased back past the pre-anneal resistance after the second anneal/aging process. FIG. **20** illustrates the results from sample P6 after several different annealing attempts. It turned out that none of the annealing methods attempted could make an ohmic contact to this lower doped p-type sample with the $W_{75}Ni_{25}$ metallization scheme deposited. Several of our attempts ended with the cut in voltage increasing which was the opposite desired effect.

P8 ($W_{90}Ni_{10}$ Metallization) (FIG. **21**) and PX ($W_{50}Ni_{50}$ Metallization) (FIG. **22**) are very similar to that of P6. No ohmic contacts were demonstrated on these the lowest doped p-type samples. In all three cases the 1000° C. Argon anneal and the 1200° C. vacuum anneal proved to be very ineffective in that they only increased the cut in voltage. However, through the auger analysis, it was anticipated to establish some possible answers to these issues. The only other question to arise was why the re-anneal lowered the cut in voltage on $W_{75}Ni_{25}$ and $W_{90}Ni_{10}$, but not $W_{50}Ni_{50}$. However, this does not matter too much because they were still not ohmic.

FIG. **23** illustrates a chart that summarizes one important aspect of the innovation directed to the new contact metallization scheme of WNi. The ohmic contact analysis at various points throughout the process is a main focus of the specification. The pre-anneal instance shows the contact formed by having WNi at the SiC interface. After annealing, the contact is dependent on the newly formed compounds of Tungsten Carbide and Nickel Silicide. After the aging process, it is dependent upon the stability of the compounds formed and whether they will continue to change structure or remain Tungsten Carbide and Nickel Silicide. These results are very pleasing especially in the cases of $W_{75}Ni_{25}$ and $W_{50}Ni_{50}$. As shown, it is to be understood that both of these compositions are stable at least unto 60 minutes of exposure to a temperature of 900° C. It will be appreciated that, this data alone can be used to support that this new contact metallization is stable enough to use in several applications.

As illustrated and described in detail supra, it is a good indication that because of the high stress in the $W_{70}Ni_{30}$, it will not make the desired optimum stable contact. However, it was not taken up to temperature and it cannot be stated for sure what an annealed sample will measure.

The stress in the W would have been acceptable, but as previously stated, W (100 at. %) makes an ohmic contact with p-type and not n-type. After further testing of W—Ni alloys, it is shown that a good, stable contact has been established. Some results have displayed just what was expected while others have not at this stage. Although more research would be done, the overall result, in terms of proving the concept of dual ohmic contact was successful.

With all of this said and the data presented, it is clear that innovation describes development of a metallization out of the ordinary. More particularly, the innovation demonstrates an ohmic contact to both n- and p-type Silicon Carbide. Though the doping level for the p-type needs to be relatively high, most conventional devices have their p-type epi-layer doped at $1\times10^{20}$ $cm^{-3}$ or higher. The findings illustrate that the new metallization can be implemented into most devices. Essentially, the innovation discloses development of a contact that is ohmic that can survive, and be stable on both n- and p-type SiC at temperatures nearing 1000° C.

It will be appreciated that the innovation can be practiced in contacts to lower doped p-type samples as well as lower doped n-type samples. Additionally, other aspects employ different W—Ni alloys, most likely ones with higher Ni concentration levels, because of the reactions desired with the SiC, and possibly some other alloys after extensive literature searches. The testing will include all of the same processing as has been set forth in detail throughout this specification.

In summary, in accordance with the innovation, it is possible to use a single metallization scheme to form ohmic contact on n- and p-type SiC, particularly in bi-polar devices where traditional approaches require utilization of different contact metallization that is exclusive of the doping. Tradi-

tional schemes are characterized by sequences of fabrication process steps that are time consuming and costly. Additionally, these traditional schemes do not support device operation as temperature increases beyond 600° C.

In accordance with aspects of the innovation, because of the ability to deposit a non-discriminatory ohmic contact metallization on both n- and p-type SiC, ion implantation and subsequent high temperature (>1100° C.) implant anneal need not be performed. It is known that conventional ohmic contact schemes employ ion implantation and high temperature implant annealing to activate the dopants, which tend to damage the layer. As evinced below, test data also shows that the non-discriminatory contact metallization on n- and p-type SiC have been tested and found stable after soaking at 1000° C. in argon for approximately 4 hours minutes.

Among others, the innovation can be employed in many scenarios including, but not limited to high temperature sensors and electronics (e.g., in excess of 600° C.) as well as high power devices. Additionally, the innovation can be employed in low-power transistors for temperatures above 300° C.

The specification describes advancements in technologies related to gas sensors, physical sensors, and silicon carbide (SiC) technology generally. In particular, the specification describes SiC as a material for advanced semiconductor electronic device applications. One advantage of this technology is that SiC electronics and sensors are capable of withstanding very hostile environments up to and exceeding 600° C. It will be appreciated that this is an advancement because most silicon (Si) based devices are limited to 350° C. maximum.

With the use of SiC, electronics will be more capable in terms of operating at higher temperatures, higher power, and even in high radiation conditions. These electronic devices could reach a large variety of areas including: aircraft, automotive, communications, power, and spacecraft industries, among others. As SiC is grown in a much more efficient way than conventionally possible, a dramatic decrease in cost, which is the main issue with SiC, can be realized.

For example, SiC-based sensors can be employed in many environments and their capabilities can include detecting hydrogen, hydrocarbons, nitrogen oxides, carbon monoxide, oxygen, carbon dioxide, etc. Clearly these capabilities offer a wide spectrum of application for an improved sensor technology. In other aspects, the innovation can be employed in the development of harsh environment physical sensors and technologies for safer aircraft and spacecraft. For example, research areas in these physical sensors include novel thin film sensors, advanced embedded sensors, and MEMS (Micro Electro-Mechanical Systems) radiation detectors, among others.

Conventional devices, however, are constrained in their ability due to the 600° C. limit. For at least this reason, the innovation discloses research in developing even higher temperature contacts (ohmic contacts) in these devices. It will be appreciated that devices capable of withstanding temperatures of about 1000° C. would have much more wide variety of application. For instance, pressure sensors in jet engines could be closer to the engines, thereby removing the delay in readings that occurs from sensing at a distance. Closer sensing would offer more reliable readings and faster response times. One factor of creating high temperature devices is creating a reliable and stable ohmic contact at the SiC interface. In accordance with the innovation, this is done with a variety of metallization schemes. The innovation can provide a stable ohmic contact at temperatures around 1000° C.

It will be understood that SiC is available in two doped types, n-type and p-type. Further, those skilled in the art will appreciate that, conventionally, a material that makes an ohmic contact with n-type will not make an ohmic contact with p-type and vice versa. An ohmic contact is defined as a metal-semiconductor contact that has a negligible contact resistance relative to the bulk or spreading resistance for the semiconductor. The innovation discloses a contact metallization that establishes a low resistance, thermally stable, ohmic contact on both n- and p-type SiC. In other words, the innovation discloses a simultaneous formation of electrical ohmic contacts to SiC semiconductor having donor and acceptor impurities (n- and p-type doping).

Additional Experimental Description

A novel tungsten-nickel ohmic contact metallization on 4H— and 6H—SiC capable of surviving temperatures as high as 900° C. is reported. Preliminary results revealed the following: i) ohmic contact on n-type 4H—SiC having net doping levels, $N_d$, of 1.4 and $2\times10^{19}$ $cm^{-3}$, with specific contact resistance $\rho_{sNd}$ of $7.69\times10^{-4}$ and $5.81\times10^{-4}$ $\Omega$-$cm^2$, respectively, after rapid thermal annealing (RTA), and $5.9\times10^{-3}$ and $2.51\times10^{-4}$ $\Omega$-$cm^2$, respectively, after subsequent soak at 900° C. for 1 hr in argon, ii) ohmic contact on n- and p-type 6H—SiC having $N_d>2\times10^{19}$ $cm^{-3}$ and $N_a>1\times10^{20}$ $cm^{-3}$, with $\rho_{sNd}=5\times10^{-5}$ and ρsNa=$2\times10^{-4}$ $\Omega$-$cm^2$, respectively, after RTA, and $\Sigma_{sNd}=2.5\times10^{-5}$ and $\rho_{sNa}1.5\times10^{-4}$ $\Omega$-$cm^2$ after subsequent treatment at 900° C. for 1 hr in argon, respectively.

Silicon carbide (SiC) sensors and electronics have been demonstrated to operate at 600° C. and 500° C., respectively. However, the need to instrument engines at higher temperatures demands more robust and reliable devices. A major impediment to such an objective is the non existence of an ohmic contact metallization scheme to SiC that can operate reliably for prolonged time periods at temperatures higher than 600° C. Rastegaeva et al. studied a W/6H—SiC (n-type) scheme up to 677° C. and reported ohmic contact, with specific contact resistivity, $\rho_s$, of between $2\times10^{-3}$ and $7\times10^{-4}$ $\Omega cm^2$.

However, time dependent evaluation was not performed to determine the long-term stability of the contacts. A report by Marinova used X-ray photoelectron spectroscopy (XPS) to investigate the interface chemistry and measured electrical contact characteristics of separate Ni based metallization on n-doped 6H—($N_d$=1-1.8×$10^{18}$ $cm^{-3}$) and 4H—SiC($N_d=10^{19}$ $cm^{-3}$) after annealing at 950° C. in nitrogen ambient. They showed that ohmic contact was formed after annealing and remained relatively stable after aging in nitrogen ambient for 100 hrs at 500° C. Kakanakova-Georgieva reported annealed WN/4H—SiC up to 1200° C. and used XPS to study the interface chemistry. The formation of $W_2C$ and $W_5Si_3$ was reported, with the contacts becoming rectifying. In the work reported by Liu et Ni/W metallization was sequentially deposited on p-type 4H— and 6H—SiC($N_a=10^{19}$ $cm^{-3}$) epilayers.

The $\rho_s$ values obtained are in relative agreement with those reported in this letter. In addition, the authors aged one of the samples (polytype not reported) in vacuum for 300 hours at 600° C. and showed slight decrease in $\rho_s$.

This letter presents the preliminary results of the investigation of W50:Ni50 alloy metallization, with the primary goal of demonstrating a simultaneous ohmic contact to both n- and p-type 4H— and 6H—SiC, in addition to achieving stability at 900° C. Ohmic contact to p-type epilayers is traditionally enhanced by ion implantation by creating a degenerately doped layer. However, this process is known to be costly and time consuming. It also induces damage to the lattice and implant activation is sometimes incomplete, thus resulting in ohmic contact degradation.

Tungsten-Nickel (W50:Ni50 at. %) alloy contacts were fabricated on commercially grown 2 μm thick homo-epitaxial

4H— and 6H—SiC epilayers of n- and p-type conductivities on high resistivity (3-11 Ω-cm) p-type substrates. For the n-type 4H— and 6H—SiC and p-type 6H—SiC, the common transfer length method (TLM) test structure was used to evaluate the contacts fabricated on the epilayer mesas. For the p-type 4H—SiC ($N_a$>2×10$^{19}$ and $N_a$=1.6×10$^{19}$ cm$^{-3}$), the metallization was fabricated directly on the epilayers without TLM structures to allow for only the qualitative evaluation of the I-V characteristics. In all cases, irrespective of the epilayer resistivity, the p-type substrates used always had a much higher resistivity than the epilayer in order to minimize substrate leakage current paths that could skew the results. The epilayer impurity concentrations were as reported by the SiC wafer vendor. The TLM structure consisted of 5 rectangular contact pads. Each sample set has three TLM subsets, with each subset having rectangular dimensions/(edge-to-edge distances) of 100×40 μm$^2$/(35, 70, 105, and 140 μm), 100×45 μm$^2$/(30, 60, 90, and 120 μm), and 100×50 μm$^2$/(25, 50, 75, and 100 μm). The TLM isolation mesas were patterned with a parallel-plate reactive ion etcher using $SF_6$ and Ar chemistry and an Al mask. The samples were solvent cleaned, immersed in equal volume of $H_2O_2$:$H_2SO_4$ solution for 15 minutes, HF for 1 minute, and followed by wet oxidation at 1000° C. to obtain an oxide layer of approximately 2000 Å. Contact vias were etched into the oxide to expose the SiC epilayer. The contact metal was then deposited from a tungsten-nickel (W50:Ni50 at. %) alloy target, patterned and etched to form the desired electrical contact to the SiC epilayers. The contact metal evaluated consisted of sputter deposited 100 nm film, followed by a 20 nm Si capping layer to prevent premature oxidation of the alloy. The samples were annealed in a Rapid Thermal Annealer (RTA) at 1000° C. for 5 sec, at a pressure of 210 mTorr, after initial argon purge. A series of current-voltage (I-V) and $\rho_s$ measurements were conducted on each TLM subset as-deposited, after RTA, and after aging over time at 900° C. in Ar ambient. Only I-V measurements were performed on non-TLM samples.

Results and Discussion

The summary results of the specific contact resistance measurements and the I-V characteristics are shown in Table 1 (Qualitative and Quantitative Electrical Characteristics of W50:Ni50 Metallization on N— and P— Type 4H— and 6H—SiC After Various Process Steps). Ohmic contact was achieved after RTA in all the subsets, except one sample set, for all the metallization runs. The $\rho_s$ values reported were obtained by averaging across the three TLM subsets from each sample. The $\rho_s$ values for the highly doped n-type 4H—SiC (>2×10$^{19}$ cm$^{-3}$) and 6H—SiC (>2×10$^{19}$ cm$^{-3}$) samples improved significantly after the RTA processes, and remained relatively unchanged after subsequent thermal treatment at 900° C. for 1 hr in argon ambient.

TABLE I

| | $\rho_s$ (Ω-cm$^2$) | | |
|---|---|---|---|
| Polytype/ Doping Level (cm$^{-3}$) | As Deposited | Post-RTA | Post 900° C., 60 min. |
| 4Hn/>2 × 10$^{19}$ | 1.7 × 10$^{-1}$ | 5.81 × 10$^{-4}$ | 2.51 × 10$^{-4}$ |
| 4Hn/1.4 × 10$^{19}$ | 1.6 × 10$^{-2}$ | 7.69 × 10$^{-4}$ | 5.9 × 10$^{-3}$ |
| 4Hp/>2 × 10$^{19}$ | Ohmic | Ohmic | Ohmic |
| 4Hp/1.6 × 10$^{19}$ | Ohmic | Rectifying | Rectifying |
| 6Hn/>2 × 10$^{19}$ | Rectifying | 5 × 10$^{-5}$ | 2.5 × 10$^{-5}$ |
| 6Hp/>1 × 10$^{20}$ | 5 × 10$^{-3}$ | 2 × 10$^{-4}$ | 1.5 × 10$^{-4}$ |

Results obtained on the p-type 6H—SiC epilayers also showed improved $\rho_s$ after 900° C. soak for 1 hr. For the two p-type non-TLM 4H—SiC epilayer samples, ohmic contact was achieved on the less doped ($N_a$=1.6×10$^{19}$ cm$^{-3}$) in as-deposited condition, but became rectifying after RTA and thereafter. However, the heavily doped sample ($N_a$>2×10$^{19}$ cm$^{-3}$) exhibited ohmic characteristics throughout, as shown in the I-V plot of FIG. **1**. In these cases, the absence of TLM structures precluded quantification of $\rho_s$. The observed $\rho_s$ increase on the lesser doped n-type 4H—SiC, and the decrease in the I-V slope of the p-type 4H—SiC after the 900° C. soaks are currently not understood. Fermi level pinning effect could only be speculated.

The W50:Ni50 alloy, upon annealing, appeared to exhibit a pseudo amphoteric ohmic contact behavior by virtue of its simultaneous ohmic contact formation on both n- and p-type SiC. It is not yet clear if this behavior could be attributed to enhanced field-emission. A report by Pelletier found the Fermi energy (FE) level to be approximately 0.29 eV above the valence band for p-type 6H—SiC having doping level of about 1×10$^{19}$ cm$^{-3}$. Also, using the effective hole mass of 1.2 $m_o$ for p-type 4H—SiC ($m_o$=1.67×10$^{-27}$ kg) from a report by Raynaud, the FE corresponding to $N_a$>2×10$^{19}$ cm$^{-3}$ was approximately 0.31 eV above the valence band. These values would suggest non-degenerate doping levels in p-type 6H— and 4H—SiC, respectively. The work functions (WF) of $W_xC_y$ compounds have been reported to be between 4.9 and 6.3 eV, which are greater than the WF of p-type 6H—SiC doped >2×10$^{19}$ cm$^{-3}$ that was reported to be about 4.85 eV. This would in principle satisfy the basic condition for $W_xC_y$ to form ohmic contact to p-type 6H—SiC, assuming the absence of interface charge pinning. Based on these arguments, it would appear that a combination of enhanced tunneling and thermionic-emission charge transport mechanisms co-exist. Conversely, nickel silicide compounds, such as reported in literature, form ohmic contacts to n-type SiC. Auger Electron Spectroscopy (AES) analyses described in detail below indicate the existence of a $W_xC_y$—$Ni_xSi_y$ composite matrix at the SiC interface after RTA. Although yet to be fully understood, the presence of $W_xC_y$ and $Ni_xSi_y$, mixtures at the n- or p-type SiC interface appears to satisfy the condition for pseudo amphoteric ohmic contact. The formation of simultaneous ohmic contact to n- and p-type SiC would have a significant impact in terms of reducing the cost and process time associated with the fabrication of SiC based bi-polar devices.

The AES depth profile of the as-deposited metallization is shown in Chart 2a. After RTA at 1000° C. for 5 seconds at 210 mTorr evacuated argon, the AES depth profile shown in FIG. **2***b* indicates that the nickel in the alloy had reacted with both the top surface Si layer and the SiC substrate to form $Ni_xSi_y$, thus freeing the carbon which reacts with tungsten. It is possible that $W_xSi_{1-x}$ was also present, although the thermodynamics favor NiSi and WC formation at 1000° C. temperature. It should be noted, however, that other analytical methods would be required to more specifically identify the carbide and silicide phases that are present at the SiC interface. The Auger depth profile after the 900° C. soak for 1 hr (Chart 2c) did not show any appreciable changes from the sample analyzed after RTA.

The preliminary results of W50:Ni50 contact metallization demonstrate ohmic contact to highly doped n- and p-type 4H— and 6H—SiC with contact resistivities shown to be stable even after thermal soak at 900° C. for 1 hr. An important aspect of these results was the observed pseudo-amphoteric ohmic contact behavior of this metallization scheme. The fundamental semiconductor physics to explain this behavior is currently being studied and would form the subject of future publication.

What has been described above includes examples of the innovation. It is, of course, not possible to describe every conceivable combination of components or methodologies for purposes of describing the subject innovation, but one of ordinary skill in the art may recognize that many further combinations and permutations of the innovation are possible. Accordingly, the innovation is intended to embrace all such alterations, modifications and variations that fall within the spirit and scope of the appended claims. Furthermore, to the extent that the term "includes" is used in either the detailed description or the claims, such term is intended to be inclusive in a manner similar to the term "comprising" as "comprising" is interpreted when employed as a transitional word in a claim.

What is claimed is:

**1**. An ohmic contact structure, comprising:

a portion of silicon carbide (SiC) that comprises an n-type SiC portion having donor impurities and a p-type SiC portion having acceptor impurities, wherein neither the n-type SiC portion nor the p-type SiC portion are subjected to degenerative doping; and

a metallization layer that simultaneously forms a dual electrical ohmic contact upon the portion of SiC, wherein the metallization layer facilitates an electrical ohmic contact to the n-type SiC portion and the p-type SiC portion.

**2**. The ohmic contact structure of claim **1**, wherein the metallization layer is stable at temperatures in excess of 600° C.

**3**. The ohmic contact structure of claim **1**, wherein the metallization layer comprises a metal carbide/silicide with a work function greater than the work function of the p-type SiC portion and a metal carbide/silicide with a work function lower than the work function of the n-type SiC portion.

**4**. The ohmic contact structure of claim **1**, wherein the metallization layer comprises an alloy of Tungsten (W) and Nickel (Ni).

**5**. The ohmic contact structure of claim **4**, wherein the metallization layer comprises a composition of W90-Ni10.

**6**. The ohmic contact structure of claim **4**, wherein the metallization layer comprises a composition of W75-Ni25.

**7**. The ohmic contact structure of claim **4**, wherein the metallization layer comprises a composition of W50-Ni50.

**8**. The ohmic contact structure of claim **1**, wherein the p-type SiC portion has a doping level greater than $2\times10^{19}$ $cm^{-3}$ p-type.

**9**. The ohmic contact structure of claim **8**, wherein the n-type SiC portion has a doping level of at least $1.4\times10^{19}$ atoms/cc n-type.

**10**. A method for establishing a dual ohmic contact to SiC having donor impurities and acceptor impurities, comprising:

combining a portion of a material having a work function greater than a work function of p-type SiC with a material having a work function lower than the work function of n-type SiC, wherein neither the n-type SiC nor the p-type SiC are subjected to degenerative doping; and

applying the material combination to the SiC having donor impurities and acceptor impurities, wherein the film establishes the dual ohmic contact.

**11**. The method of claim **10**, wherein the material combination forms a film.

**12**. The method of claim **10**, wherein the material having a work function greater than the work function of p-type SiC is Tungsten Carbide.

**13**. The method of claim **11**, wherein the material having a work function lower than the work function of n-type SiC is Nickel Silicide.

**14**. The method of claim **12**, wherein the combination of W and Ni is one of W90-Ni10, W75-Ni25, or W50-Ni50.

**15**. The method of claim **10**, further comprising doping a portion of the SiC having donor impurities at a level of at least $1.4\times10^{19}$ $cm^{-3}$ n-type.

**16**. The method of claim **14**, further comprising doping a portion of the SiC having acceptor impurities at a level of at least $2\times10^{19}$ $cm^{-3}$ p-type.

**17**. The method of claim **10**, wherein tungsten silicide is observed at the silicon carbide interface.

* * * * *